Marine Geophysical Research (2023) 44:6
https://doi.org/10.1007/s11001-023-09514-3

ORIGINAL RESEARCH PAPER

Reading the sediment archive of the Eastern Campeche Bank (southern Gulf of Mexico): from the aftermath of the Chicxulub impact to Loop Current variability

Christian Hübscher[1] · Tobias Häcker[1] · Christian Betzler[2] · Claudia Kalvelage[1,3] · Benedikt Weiß[1,4]

Received: 3 February 2023 / Accepted: 6 March 2023 / Published online: 21 March 2023

Abstract

This is the first high-resolution seismic study showing how the Chicxulub impact shaped the eastern slope of the Campeche Bank in the south-eastern Gulf of Mexico. The induced shock wave fractured Cretaceous strata causing the collapse of the upper slope and shelf over a length of ca. 200 km. Failed material was either transported downslope or remained in parts on the accommodation space created by the collapsed. In the Cenozoic, the East Campeche Plastered Drift developed within the created accommodation space, controlled by the inflowing surface current from the Caribbean, which forms the Loop Current. The internal reflection configuration of the drift shows that the closure of the Suwannee Strait in the Late Oligocene and the closure of the CAS in the Mid to Late Miocene controlled the variability of the southern Loop Current in time. Since the Loop Current transports heat and moisture from the western Atlantic warm water pool into the North Atlantic and further to NW Europe by the Gulf Stream, the drift represents an archive for controlling factors that influenced climate of the northern hemisphere. This first high-resolution seismic reflection study from the eastern Campeche Bank expands the understanding of destructive processes that a meteorite impact induces into the earth system. Furthermore, these data document that the East Campeche Plastered Drift bears the potential to understand the link between the climate variability of the northern hemisphere and oceanic processes in the equatorial western Atlantic.

Keywords Marine reflection seismics · Plastered drift · Deep base level · Paleoceanography · Meteorite impact · Pockmarks

✉ Christian Hübscher
christian.huebscher@uni-hamburg.de

Tobias Häcker
Haecker.Tobias@web.de

Christian Betzler
Christian.Betzler@uni-hamburg.de

Claudia Kalvelage
ClaudiaKalvelage@hotmail.com

Benedikt Weiß
Benedikt.Weiss@bsh.de

[1] Center for Earth System Research and Sustainability, Institute of Geophysics, University of Hamburg, Bundesstraße 55, 20146 Hamburg, Germany

[2] Center for Earth System Research and Sustainability, Institute of Geology, University of Hamburg, Bundesstraße 55, 20146 Hamburg, Germany

[3] Present Address: Die Fähre, Hamburg, Germany

[4] Present Address: Bundesamt für Seeschiffahrt und Hydrografie, Hamburg, Germany

Introduction

The impact of the Chicxulub meteorite responsible for the Cretaceous-Paleogene (K-Pg) extinction event occurred 66 Ma ago on the present-day coastline of Mexico on the northern Yucatán Platform in the southern Gulf of Mexico (GoM; Fig. 1) (Alvarez et al. 1980; Hildebrand et al. 1991; Schulte et al. 2010). The energy introduced into the Earth system by the impact was partially converted into a shock wave that would be comparable to the consequences of a magnitude 11–12 earthquake (Day and Maslin 2005). The shock wave reached the Florida coast within 4 min, triggering surface waves with amplitudes of one meter (Poag 2017). Portions of the carbonate platforms collapsed, carrying an estimated 1.98×10^5 km^3 of sediment into the Gulf Basin (Sanford et al. 2016). The impact crated an elongated, up to 490 m deep basin the stretched from the crater to the northern Campeche shelf break, hence separating the Yucatan Platform in an eastern and western part (Guzmán-Hidalgo et al. 2021).

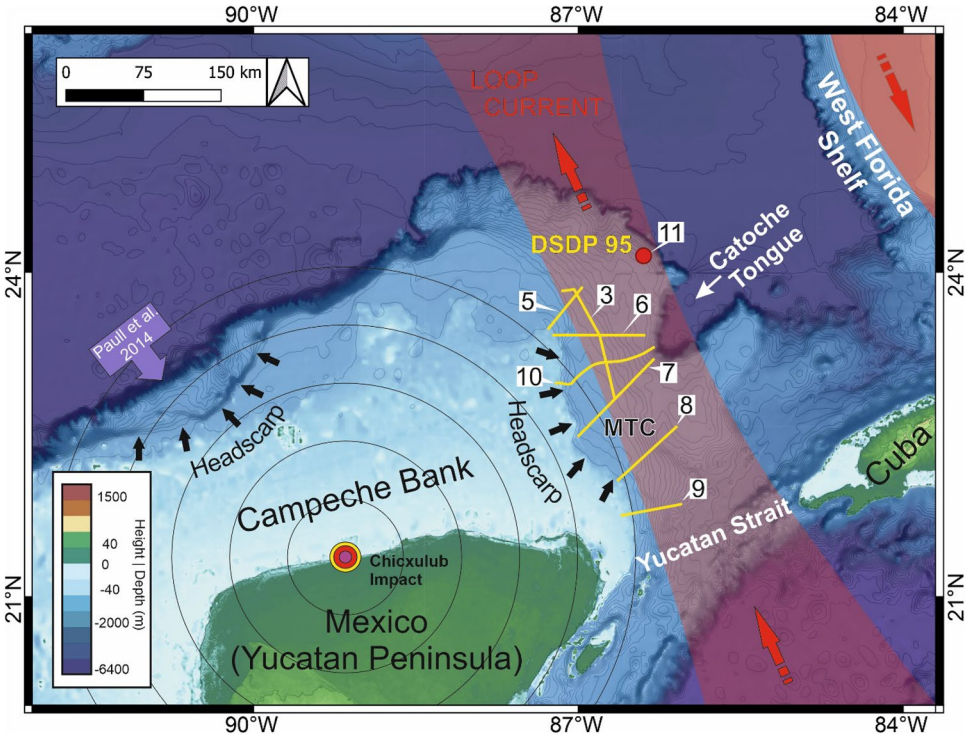

Fig. 1 Bathymetric map of southern Gulf of Mexico with adjacent Yucatan and Florida straits. The yellow lines mark the seismic profiles, the label indicate the figure numbers. MTC: mass transport complex. The location of the Chicxulub impact crater is indicated according to Paull et al. (2014). Concentric rings indicate the impact induced seismic wave

Overall, the K-Pg boundary deposits (KPBD), comprising melt rock, suevite, and lithic impact breccia, represent the largest mass wasting sedimentary unit of the Earth (Sanford et al. 2016; Poag 2017) which triggered tsunamis along the GoM (Kinsland et al. 2021). The northern Campeche Bank, a cretaceous carbonate platform, is the closest present-day Cretaceous-Paleogene (K-Pg) boundary outcrop to the Chicxulub impact structure (Paull et al. 2014). The authors used multibeam data for describing impact related mass wasting due to seismic shaking produced by the impact. The arcuate steep escarpment face of the northern Campeche Bank (black arrows in Fig. 1) represents the headscarp left behind by extensive debris flows, which are found in wide areas of the GoM. Hübscher and Nürnberg (2023) proposed that the arcuate escarpment at the eastern Campeche Bank (ECB) represents a similar headscarp created by Chicxulub impact related mass wasting.

As summarized by Mullins et al. (1987), ocean currents in the eastern GoM today are dominated by the Loop Current. This surface current which flows from the Caribbean Sea and through the Yucatan Strait, streams clockwise into the eastern Gulf and exits into the Atlantic via the Florida Strait. The surface current then flows northward, where it joins the Antilles Current northwest of the Bahamas and accounts for about one-third of the total volume of the Gulf Stream system. Because the Loop Current transports warm tropical water from the Caribbean to high northern latitudes (Oey 2008 and references therein), its temporal variability has been an important controlling parameter for Northern Hemisphere climate. Loop Current variability since the Late Cretaceous has been reconstructed from seismic and sedimentological data from the western Florida shelf by Gardulski et al. (1991) (Fig. 2). Comparable studies from the conjugate ECB are lacking. This is significant because until the closure of Suwannee Strait in the late Oligocene to early Miocene, surface flow was northward in both the east and west. Subsequently, the Loop Current formed and the flow along the western Florida shelf was southward, in contrast to the eastern Campeche Bank (ECB).

In this study, we use high-resolution reflection seismic data measured during RV METEOR Expedition M94 (Hübscher et al. 2014) to reconstruct the consequences of the Chicxulub impact on the upper slope of the ECB, as well as the influence of the changing oceanic current regime like the Loop Current on the deposited sediments after the impact.

Setting

Geology of southeastern GoM

Legacy seismic data and cores collected on Leg 77 of the Deep Sea Drilling Project (DSDP) provide a broad history of the geology of the southeastern GoM (Schlager et al. 1984). Drill cores from several knolls in the deep southern GoM, i.e., positive bathymetric features with little overburden over crystalline basement, reveal that Paleozoic basement is comprised of rifted continental crust (Buffler et al. 1984). The

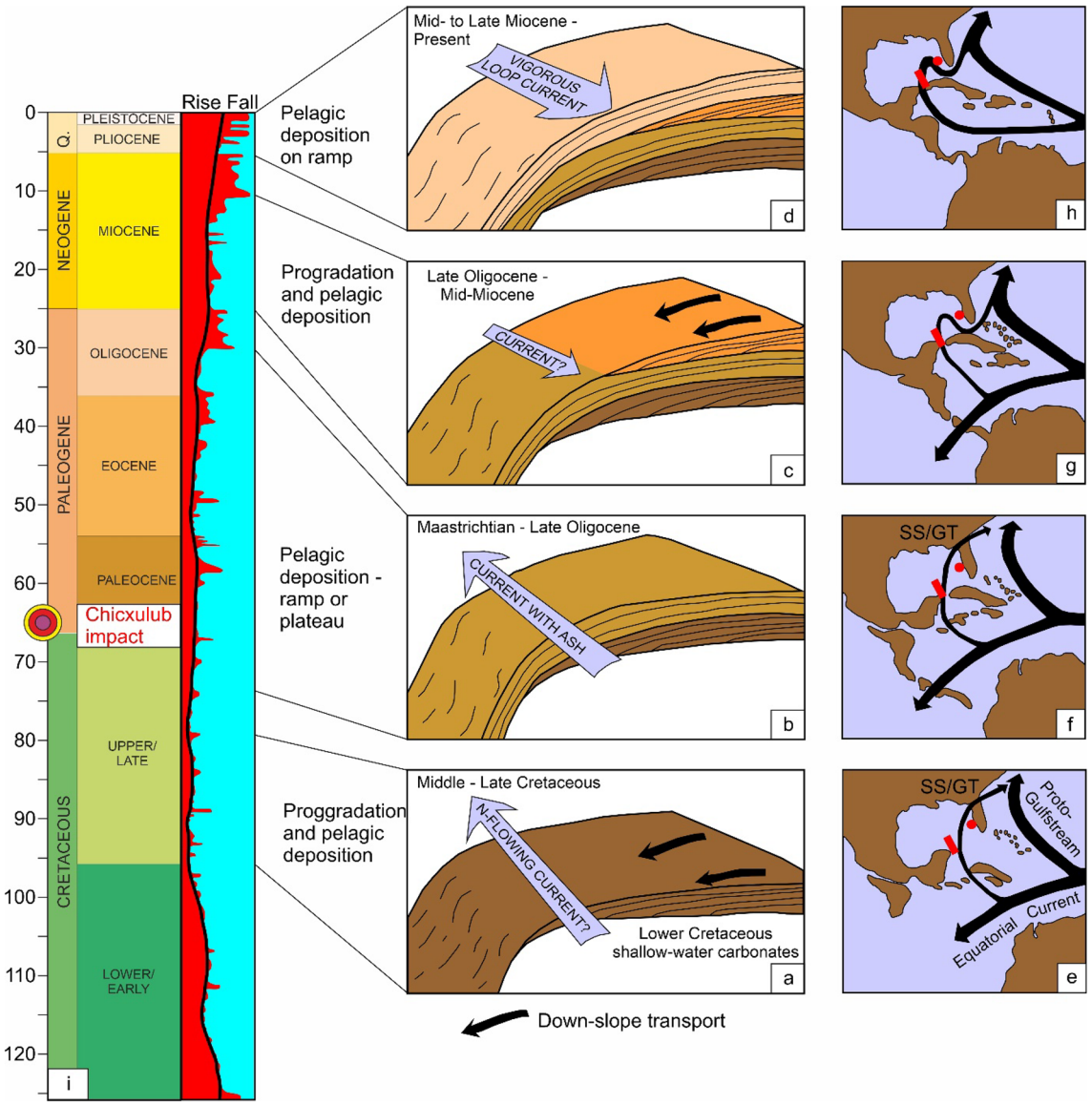

Fig. 2 Conceptual sketch showing the four major depositional systems identified by Gardulski et al. (1991) in the context of paleo-circulation (a-h) and eustasy (i). Red dot in paleo-cirulation maps indicate study area of Mullins et al. (1988) and Gardulski et al, (1991). Red rectangle indicates working area of this study. GT: Gulf Trough; SS: Suwannee Strait

extent and nature of this transitional crust is still subject of controversy (Kneller and Johnson 2011; Mickus et al. 2009; Pindell and Kennan 2009; Christeson et al. 2014; Eddy et al. 2014; van Avendonk et al. 2015), as no basement material has been recovered from deep portions of the basin and it is poorly resolved on the data used by Schlager et al. (1984).

Campeche Bank

The Campeche Bank north of the Yucatan Peninsula (also known as Yucatan Shelf or Yucatan Carbonate Platform) in the GoM is a carbonate bank which evolved until the mid-Cretaceous (Ordonez 1936). It is considered as geologically similar to the southern Florida platform (Antoine and Ewing 1963; Uchupi and Emery 1968). As summarized by Guzmán-Hidalgo et al. (2021), the Mesozoic and Cenozoic succession comprises mainly carbonate and evaporite, as well as minor red bed siliciclastic rocks at the base.

The Campeche Bank is characterized by a gently dipping seafloor, down to 120 m, followed by a locally 60 km wide terrace down to ca. 400 m, from where it plunges to 3000 m. Two submarine terraces (30–36 m, 50 – 63 m) occur in the shallow part, with minor reefs growing at the position of the deeper terrace (Purser 1983).

The lower slope of the northwestern (Site 86), northern (Site 94) and northeastern (Site 96) of the Campeche Bank

has been drilled in the course of DSDP Leg 10 back in 1970 (Fig. 2; Worzel et al. 1973). The results derived from spot coring indicated that the Bank grew as a massive carbonate platform since Cretaceous times. No evidence for any reef structures or barriers has been reported. With the exception of Cretaceous dolomite, the recovered sediments were of deep-water origin (bathyal depths), indicating that the bank has been in the same relative environment since at least Paleocene or Late Cretaceous. In the context of DSDP Leg 10, Worzel et al. (1973) interpreted the steep upper slope of the northern Campeche Bank as the result of upbuilding carbonate sediments. The authors ruled out to see the escarpment as a fault scarp or as the detrital accumulation seaward of a barrier or reef complex.

The Lower Paleocene chalks drilled on close to our study area at Site 95 in a water depth of 1663 m are fractured. Discontinuities in the section and unconformities observed in the seismic data were interpreted to result from slumping that occurred throughout the Cenozoic along the ECB slope (Worzel et al. 1973). As it is typical for a ramp, shallow water sedimentary facies are arranged into depth dependent belts with red and green algae, molluscs, gastropods and foraminifers down to 80 m, and finer grained deposits in deeper waters (Logan et al. 1969).

Chicxulub impact

The energy input into the Earth system by the Chicxulub at the Cretaceous-Paleogene (K-Pg) boundary is estimated to be $4.2–12 \times 10^{20}$ kJoule (Covey et al. 1994; Hildebrand et al. 1998). As summarized by Sanford et al. (2016) the subsequent magnitude 11 earthquake generated seismic shaking, ground roll and a mega-tsunami wave train (Kinsland et al. 2021) that travelled across the gulf within an hour. The resulting debris flows redistributed about 2×10^5 km^3 carbonate sediments in the entire GoM, mainly from the Texas shelf and Florida Platform (Sanford et al. 2016). The redeposited carbonate debris observed in seismic and borehole data by Sanford et al. (2016) at the Cretaceous-Paleogene boundary has thicknesses on decimeter and hectometer-scale. Poag (2017) used seismic reflection profiles from the West Florida Shelf to investigate impact-induced seismic shaking, strata disruption and subsequent erosion of the Maastrichtian-Campanian depositional sequence.

Paull et al. (2014) discussed catastrophic mass wasting along the northern Campeche Bank due to seismic shaking triggered by the Chicxulub impact (Fig. 1). The gravity flows contributed to what Paull et al. (2014) called the "K-Pg Cocktail deposits", comprising melt rock, suevite, and lithic impact breccia. The mass failure created a rather flat an up to 50 km wide basal shear surface ramp, on which the Cocktail deposits were deposited, later covered by Cenozoic post K-Pg event deposits. Guzmán-Hidalgo et al. (2021) showed later, that the flank collapse at the upper slope of the northern Campeche Bank (Fig. 1) occurred at the northern end of the impact basin that stretches from the shelf break to the crater.

The processes important to this study are thus: (1) Within the first seconds to minutes after impact, seismic ground roll caused sediment liquefaction and internal fracturing of the upper Cretaceous deposits (Day and Maslin 2005; Poag 2017). The northern margin of the Campeche Bank collapsed. (2) Turbidite flows triggered by tsunamis within the first few hours after impact are deposited in the GoM and Caribbean (Sanford et al. 2016). (3) Carbonates suspended in the water and iridium-rich ejecta rocks deposited within the first days to weeks after impact (Sanford et al. 2016). Hübscher and Nürnberg (2023) speculated that the eastward concave, arcuate rim of the Campeche Bank represents the headwall domain of an about 150 km broad mass transport complex (MTC), triggered by the Chicxulub impact.

Tectonics, currents and climate

The interaction between tectonics and oceanography north of the Yucatan Strait has been described for the western Florida shelf (Mullins et al. 1988; Gardulski et al. 1991; Fig. 2). After the mid-Cretaceous drowning of the Florida platform sediment gravity flows caused prograding deposition under the additional influence of a northbound contour current (Fig. 2a, e). Starting in the Maastrichtian, pelagic deposition of mainly carbonate ooze continued for about 40 Myrs. (Fig. 2b). Until then, the northbound current exited the GoM through the Suwannee Straight until early Eocene and through the Gulf Trough to late Oligocene (Fig. 2e, f). The transition from Late Cretaceous-Paleogene aggradation to late Oligocene-middle Miocene progradation was contemporaneous with the infilling and closure of the Suwannee Strait and Florida Trough during falling eustatic sea level (Fig. 2c, g, i) (Gardulski et al. 1991). In the following deposition took place under the influence of the southward flow of the emerging Loop Current. It should be noted that this change in flow direction did not affect the ECB to the west.

The closure of the Central American Seaway (CAS) caused a significant intensification of the Loop Current vigor (Fig. 2d, h), but the timing of this event is debated. Although the Isthmus of Panama as a land bridge formed around 2.8 Ma (O´Dea et al. 2016), massive interoceanic seawater exchange between Atlantic and Pacific ceased by 9.2 Ma due to collision related uplift (Newkirk and Martine, 2009; Osborne et al. 2014).

Subsequently an aggradational ramp developed on the western Florida Shelf above the Mid-Miocene unconformity (MMU; Mullins et al. 1987; 1988), consisting mostly of calcareous pelagic sediments with some input from the

Mississippi River (Fig. 2i). Gardulski et al. (1991) that the strong, southward directed current blocked off-platform transport, because the Loop Current reached down to the sea floor, e.g. due to the mid-late Miocene sea level fall (Fig. 2i).

Hübscher et al. (2010) used sediment subbottom profiler data from the southeastern GoM and discussed the influence of the northbound Loop Current and the counter flow on sediment drift depositions on the ECB and West Florida Shelf. The data resolved a prominent unconformity at the upper slope up to 20 m below sea floor which was interpreted as the consequence of a significant flow change sometime during the Pleistocene. Hübscher and Nürnberg (2023) interpreted additional hydroacoustic and geological data collected during RV METEOR expedition M94 (Hübscher et al. 2014) and attributed that unconformity and its correlated conformity to the Mid-Pleistocene Transition (MPT). The data provided several indications that the Loop Current weakened after the MPT hence contributing to the further cooling of the Northern hemisphere. Cold-water corals with drift complexes developed on the upper slope, first described by Hübscher et al. (2010).

Material and methods

During RV METEOR expedition M94 in 2013 we collected high-resolution seismic reflection data by means of two GI-Guns and a short 16-channel analog streamer with a group interval of 6.25 m (Hübscher et al. 2014). The volume of each GI-Gun was 45 in^3 for the generator with a 105 in^3 injector volume, both operated in “true GI” mode. The weather conditions were rather harsh, so noise level was high. The undamped passband of the frequency filter was between 20 and 200 Hz. Further processing steps included predictive deconvolution, spherical divergence correction, stacking, time-migration, white-noise suppression by the technique described by Butler (2012) as implemented in Schlumbergers VISTA® processing package and fx-deconvolution. For more details about the marine seismic method see Hübscher and Gohl (2014). Additionally, we used vintage seismic profiles GT2-16 and GT3-62 collected in the course of the Gulf Tectonics projects by the University of Texas Institute for Geophysics (Buffler 1977; Worzel and Buffler 1978; Dillon et al. 1979). IHS Markit provided the Kingdom® Geophysics software for data interpretation. The vertical exaggeration which is given for each seismic figure has been calculated with a constant velocity of 1800 m/s, which is the velocity that has been estimated by Hübscher and Nürnberg (2023) for upper strata.

Observations

As noted already by Hübscher and Nürnberg (2023), the ECB between 22° and 23,5° north forms a nearly 200 km long arcuate terrain step, which was interpreted as the headscarp of a mass transport complex (MTC; Fig. 1). The upper slope in water depth between 300 and 600 m reveals a terrace-like morphology. Between 600 to 1000 m the isobaths are convex-shaped downslope.

In order to set up a seismo-stratigraphic framework we first chose the M94 profile in Fig. 3 which runs approximately along the contour and exhibits all the here defined seismic units. The term "seismic unit" (or simply "unit") is purely descriptive for intervals with similar internal reflection configurations bounded by unconformities or conformities atop and at their base. The identified eight units, labelled bottom up ECB1-8 (ECB: East Campeche Bank), are listed and characterized in Fig. 4. The profile in Fig. 3 represents also the tie or anchor profile from which the stratigraphy is extrapolated to the dip profiles in Figs. 5, 6, 7. No tie lines are available for the southern two profiles in Figs. 8 and 9 which are quite close to the Yucatan Strait (Fig. 1), where northbound currents from the Caribbean into the Gulf of Mexico are strongest (Sheinbaum et al. 2002). The lower three units can be identified by jump correlation, the units above are described in a general way. After establishing the seismo-stratigraphic scheme for the M94 seismic data, the scheme was projected on the vintage seismic data (Fig. 10).

The lowest unit ECB1, identifiable in the profiles of Figs. 3, 6, 9 and 10, exhibits faint subparallel and parallel reflections. The upper bounding unconformity is irregular and truncated. The resulting ramps have steps of about 100 ms TWT, corresponding to at least 100 m if a p-wave velocity of 2 km/s is assumed. The base of ECB1 could not be imaged.

The upper boundary of the overlying unit ECB2 represents an irregular or wavy conformity where it is not truncated. Internal reflection patches are wavy but discontinuous, other segments reveal a chaotic pattern. ECB2 comprises a TWT interval of up to 140 ms, representing 140 m if a seismic velocity of 2 km/s is assumed. Unit ECB2 and the units above in the MTC terminate upslope against the arcuate headscarp (Figs. 5, 6).

Chaotic reflections of low amplitudes with some intercalated high amplitude reflections characterize unit ECB3, which comprises a TWT interval of up to 60 ms (ca. 60 m). In the northern profiles this unit fills up depressions in the top of ECB2 (Figs. 5, 6). In the center of the MTC, ECB3 is thickest (Fig. 7). ECB terminates downslope against a buttress formed by ECB1/2 in Figs. 7, 9 and 10. In Fig. 9, however, ECB3 overran the buttress. In the central part of the study area and close to the buttress, internal and partly upslope diverging reflections and thrusts are truncated by

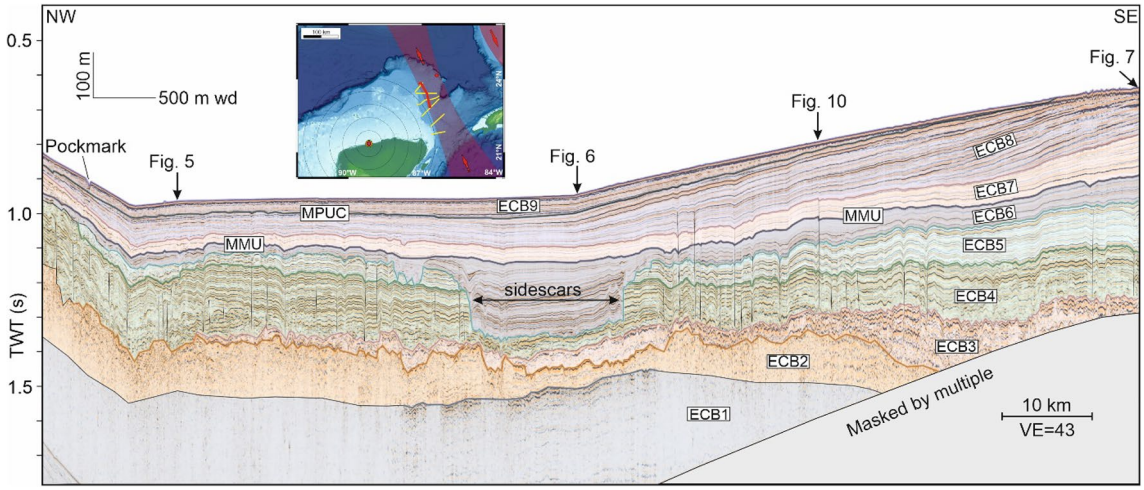

Fig. 3 Contour parallel M94 seismic reflection profile. Arrows indicate crossing dip profiles. The profile location is drawn in the insert map as red line. Seismo-stratigraphic units are labeled ECB1-9 (East Campeche Bank). MPUC marks the Mid Pleistocene unconformity and correlated conformity according to Hübscher and Nürnberg (2023). MMU: Mid Miocene Unconformity. A clean version of the seismic profile is shown in Fig S1

Fig. 4 Overview about seismo-stratigraphic scheme. lK: Lower Cretaceous; uK: upper Cretaceous; Pg: Paleogene; Pa: Paleocene; uOl: upper Oligocene; Mio: Miocene; mMio: middle Miocene; MMU: Mid-Miocene Unconformity; MPT: Mid-Pleistocene Transition; MPUC: Mid-Pleistocene Unconformity / Conformity

Seismic Example	Seismic Unit	Reflection Configuration	Stratigraphy	Interpretation
	ECB9	Prograding onlapping clinoform, parallel to divergent, continuous, high amplitude	MPT-Present	Raising deep base level (Loop Current attenuation)
	ECB8	Prograding, partly offlapping clinoform, parallel to divergent, continuous,high amplitude	MPUC MPT-mMio	Falling deep base level (strong Loop Current)
	ECB7	Prograding clinoform, parallel to divergent, continuous reflections of low to medium amplitude		Incerasing current control (Loop Current)
	ECB6	Aggrading, subparallel to wavy, continuous reflections of high amplitude	MMU Mio	Infilling sheeted drift
	ECB5	Prograding, subparallel to wavy, continuous reflections of low amplitude	uOl-Mio	No to little current control, off-bank transport
	ECB4	Aggrading, subparallel to wavy continuous reflections of high amplitude	Pa-uOl	No to little current control, no off-bank transport
	ECB3	Mainly low amplitudes, chaotic, some intercalated high amplitude reflections	K-Pg	Remobilized by L-Pg impact ('K-Pg cocktail')
	ECB2	Wavy patches or chaotic, low to medium amplitudes, discontinuous	uK	Overprinted, fractures by K-Pg impact ('shaken and stired')
	ECB1	Subparallel, aggrading and continuous, medium amplitudes, upper boundary truncated	lK	Carbonate plattform

the overlying unit (Figs. 7, 10). As Fig. 8 shows, ECB3 is also present at the lower slope. No buttress is present here.

ECB4 reveals continuous and subparallel to wavy reflections of high amplitude, which build a mainly aggrading unit. The maximum TWT interval of up to 200 ms may represent a thickness of 200 m or less. If 1.8 km/s, which Hübscher and Nürnberg (2023) calculated for the upper strata, are taken for depth conversion, the 200 ms TWT correspond to 180 m. ECB5 and ECB6 overly ECB4 over wide areas concordantly. However, some areas are truncated or missing (Figs. 3, 5, 6, 10). In the slope parallel profile (Fig. 3) over 17 km in length, the upper ca ¾ part of unit

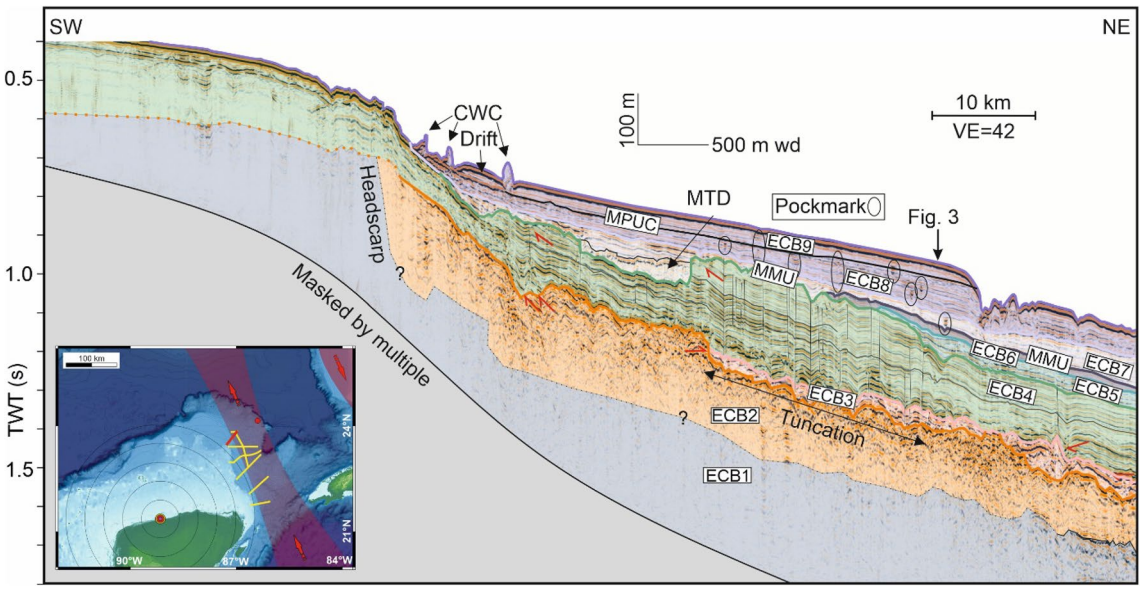

Fig. 5 Northernmost M94 seismic reflection profile outside the ECPD (East Campeche Plastered Drift). Cold-water coral (CWC) and the small drift according to Hübscher et al. (2010). The profile location is drawn in the insert map as red line. The black arrow marks the crossing location of profile in Fig. 3. MTD: Mass transport deposit. For other abbreviations see Fig. 3. A clean version of the seismic profile is shown in Fig S2

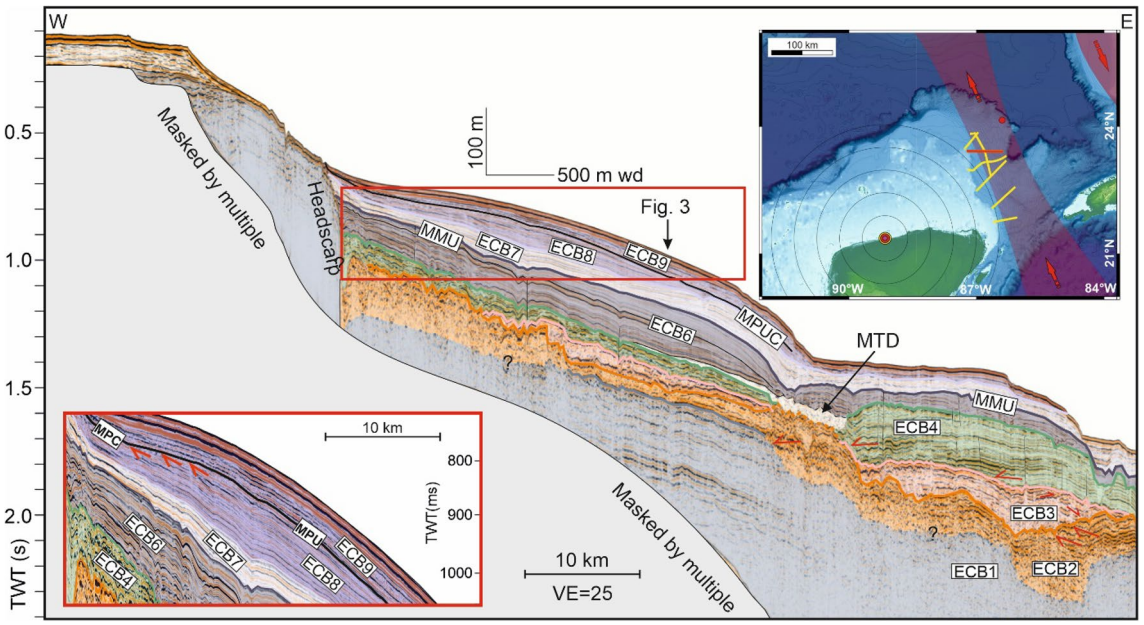

Fig. 6 M94 seismic reflection profile across the northern end of the ECPD. The profile location is drawn in the insert map as red line. Red arrows mark reflection terminations. The black arrow marks the crossing location of profile in Fig. 3. MTD: Mass transport deposit. For other abbreviations see Fig. 3. A clean version of the seismic profile is shown in Fig S3

ECB4 are eroded. The side walls of the erosional feature are near vertical. The dip profile in Fig. 6 across this depositional gap shows that unit ECB4 is rather thin if compared to the profiles to the north and south. In the same profile, unit ECB4 thickens again where the slope forms an almost horizontal plateau.

The internal reflection configuration of ECB5 is similar to that of ECB4, but reflection amplitudes are generally lower compared to ECB4, and it reaches its maximum thickness

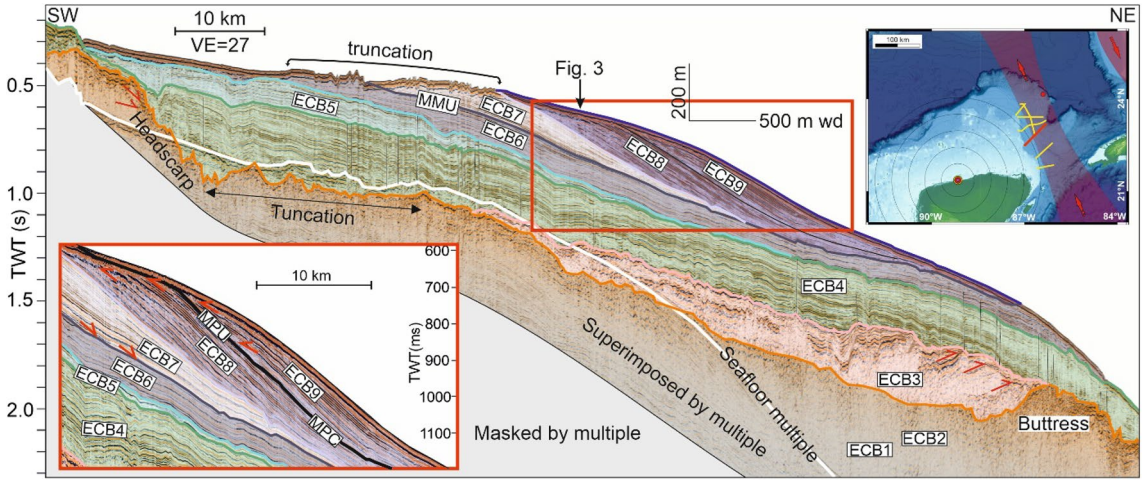

Fig. 7 M94 Seismic reflection profile across the central ECPD. The profile location is drawn in the insert map as red line. The black arrow marks the crossing location of profile in Fig. 3. Red arrows mark reflection terminations. For other abbreviations see Fig. 3. A clean version of the seismic profile is shown in Fig S4

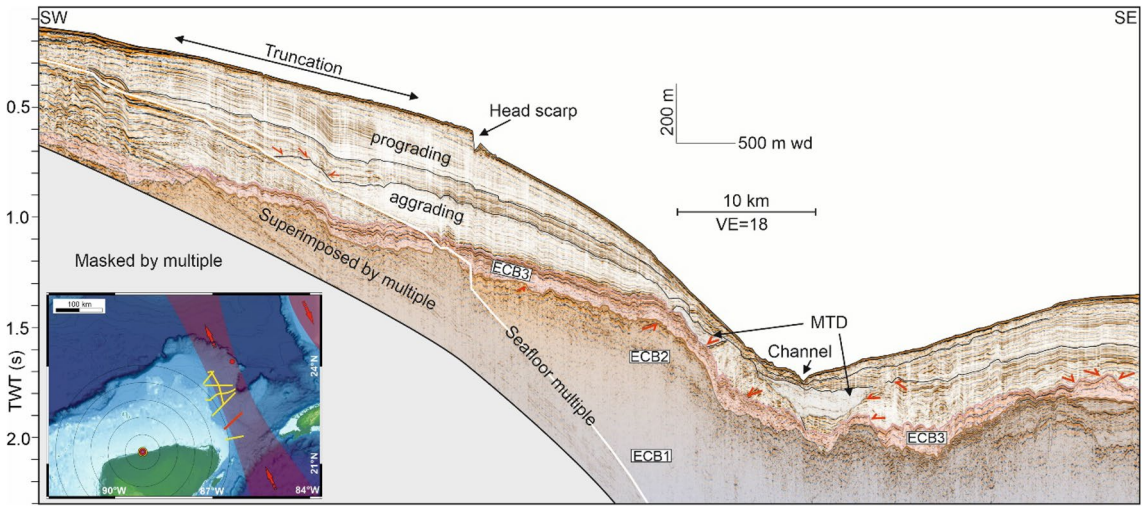

Fig. 8 M94 seismic reflection profile across the southern ECPD. ECB1-3 are identified from jump correlation. MTD: Mass transport deposit. The profile location is drawn in the insert map as red line. Red arrows mark reflection terminations. For other abbreviations see Fig. 3. A clean version of the seismic profile is shown in Fig S5

on the upper slope and in Fig. 7, where ECB5 is prograding. North and south of the profile in Fig. 7, unit ECB5 is either absent or condensed, which means it is too thin to get resolved by the seismic data.

ECB6 is aggrading. Internal reflections are subparallel to wavy. ECB6 fills the missing ECB4 packages (Fig. 3, 5, 6) and comprises up to ca. 200 ms TWT (ca. 180 m) where it fills the eroded of ECB3 in Fig. 3. The upslope termination of ECB6 is truncated in a water depth of ca. 350 m (400 ms TWT). Near-vertical faults, possibly just narrow folds if considering the limited lateral resolution, are abundant within unit ECB4, some of them correlate downwards with the top of the underlying unit ECB3 (Fig. 5–7), other propagate into units ECB5 or ECB6.

Internal reflections of the prograding clinoforms deposits of ECB7 are continuous and parallel to divergent. The reflection amplitudes are low to medium. Its thickness may increase (Fig. 5) or decrease (Fig. 7) downslope. In Fig. 7, the upslope end of ECB7 is truncated at ca. 350 m (450–500 ms TWT).

The appearance of ECB8 varies along slope. In the northernmost profile (Fig. 5), the internal reflections are straight and slightly diverging downslope, and some small depressions are intercalated. Reflection amplitudes within

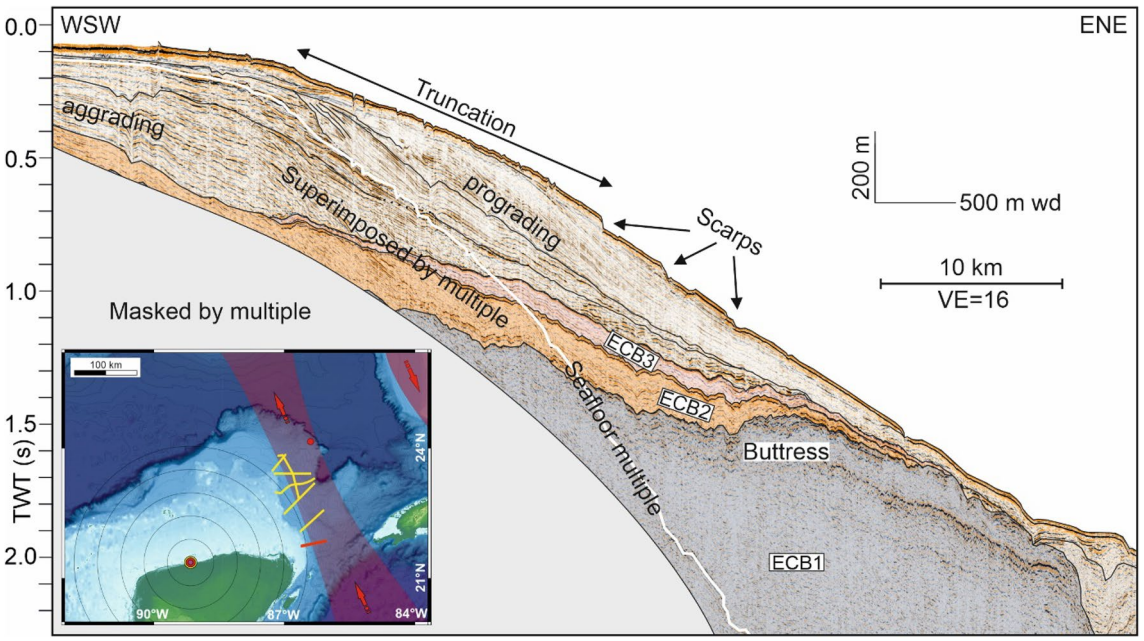

Fig. 9 Southernmost M94 seismic reflection profile south of the ECPD and close to the Yucatan Strait. ECB1-3 were identified by jump correlation. For other abbreviations see Fig. 3. A clean version of the seismic profile is shown in Fig S6

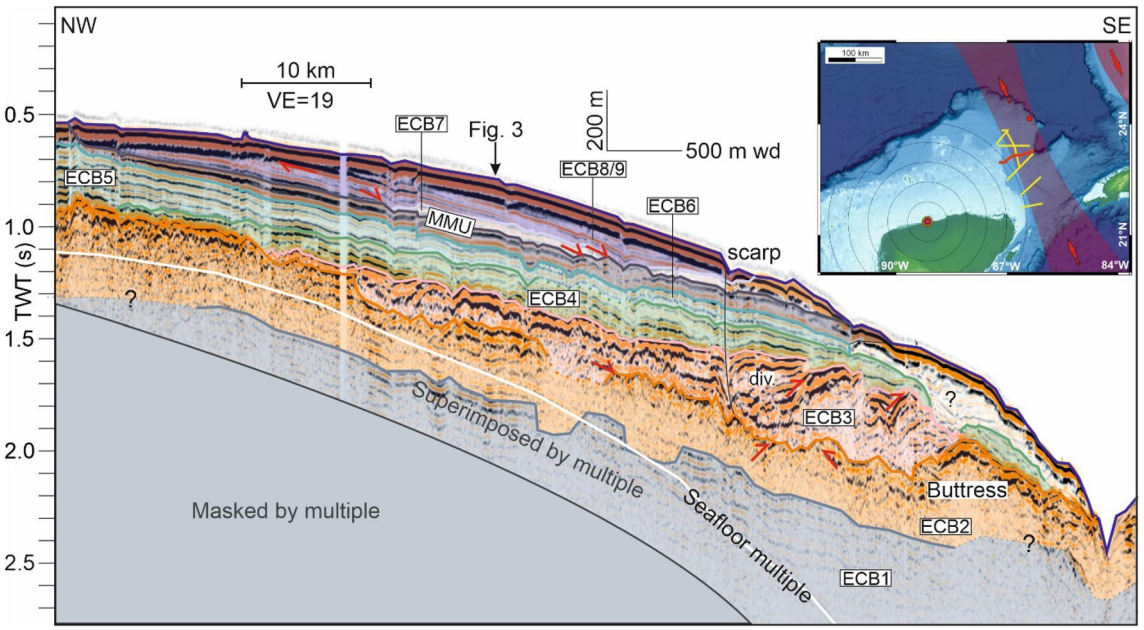

Fig. 10 Vintage seismic reflection profile GT3-62 (Buffler 1977) across the central ECPD used for jump correlation from DSDP Site 95. The black arrow marks the cossing location of profile in Fig. 3. For other abbreviations see Fig. 3. A clean version of the seismic profile is shown in Fig S7

these depressions are higher than beside of them. Along this profile, ECB8 thickens from ca. 90 m (100 ms TWT, v = 1.8 km/s) to ca. 180 m (200 ms TWT, v = 1.8 km/s). In Figs. 6 and 10, unit ECB8 represents a ca. 90 m thick (100 ms TWT, v = 1.8 km/s) mounded structure at the upper slope. In Fig. 7, unit ECB8 forms sigmoidal clinoform with offlapping, down stepping reflections. Here, ECB8 reaches its maximum thickness of ca. 200 m (220 ms TWT, v = 1.8 km/s).

Unit ECB9 is separated from ECB8 by the Mid Pleistocene unconformity and correlated conformity (MPUC), which has been described with sediment subbottom profiler data in Hübscher and Nürnberg (2023). The M94 seismic data resolve MPUC and unit ECB9 only in Figs. 5–7. In the northernmost M94 seismic profile, the internal reflections of ECB 9 are parallel. The transition from the Mid Pleistocene unconformity (MPU) to the correlated conformity (MPC) occurs at 810 ms TWT, marked by the most basinward toplap of ECB8 against the MPUC (blowup in Fig. 6). Upper ECB9 clinoforms onlap the MPU from 840 ms TWT and above in Fig. 7.

Since the profiles in Fig. 8 and 9 are not linked to the profiles further north by a tie profile, the extrapolation of ECB4-8 to these profiles is not possible. However, both profiles reveal the transition from aggrading to prograding above unit ECB3. The upper slope is truncated in both instances down to 450 m water depth (600 ms TWT, v = 1.5 km/s).

Interpretation and discussion

Stratigraphic constrains from DSDP Site 95

To constrain the stratigraphic interpretation of lower units ECB1-3, two steps were taken. First, we scaled the GT2-16 profile and a section of DSDP Site 95 pre-site data (Worzel et al. 1973) the same and plotted them against each other (Fig. 11). The quality and vertical resolution of the two data are different, so few conclusions can be drawn. One important result is that the Cretaceous-Paleocene boundary can be identified and that ECB1-2 corresponds to Lower Cretaceous strata and ECB3 to Upper Cretaceous strata. Jump correlation by comparing unconformities and internal reflection patterns of the profiles in Figs. 10, 11 across the Catoche tongue (Fig. 1) allows the temporal placement of units ECB1-3 in the ECB.

A second jump correlation was required to identify ECB1-3 in the southern profiles (Figs. 8, 9) of Fig. 7. Because the previously described ECB4-8 seismic units exhibit considerable variability above 1500 m water depth (2 s TWT), no further correlation is proposed between the Cenozoic stratigraphy of Site 95 and the seismic data in Fig. 11.

The Campeche Carbonate Platform and the Chicxulub impact

Unit ECB1 represents the acoustic basement and is imaged best in Fig. 10. According to DSDP Site 95 this unit comprises shallow carbonates of the Campeche Bank. The chaotic and discontinuous reflection characteristics of ECB2 corresponds with the Selma-Pine Key depositional sequence on the west Florida Shelf (Randazzo 1997), which seismic signature Poag (2017) interpreted as the direct consequence of seismic shaking and ground roll by the nearby Chicxulub impact. Poag (2017) coined the term "shaken and stirred" for this unit. In fact, Worzel et al. (1973) already noted that the Lower Paleocene chalks drilled at Site 95 in a water depth of 1663 m are fractured with many of the fractures annealed.

The amphitheater like headscarp on the ECB and its similarity to the headscarp at the northern Campeche Bank (Figs. 1, 5, 6, 7) corroborates the interpretation that also the ECB was structurally overprinted by the impact. When adopting the conceptual model by Paull et al. (2014; their Fig. 5), then it was the seismic wave from the impact that resulted in the collapse of the ECB ca. 200 km along the platform rim. According to Paull et al. (2014), parts of the failed material was transported into the basin by gravity flows. Some part of this mass transport deposits (MTD) remained on the decollement. The abbreviation MTC (mass transport complex) in Fig. 1 refers to the combined MTD deposits on the upper slope within the created accommodation spacem and the exported MTD of the lower slope. Unit ECB3 reveals several characteristics of an MTD (e.g., Bull

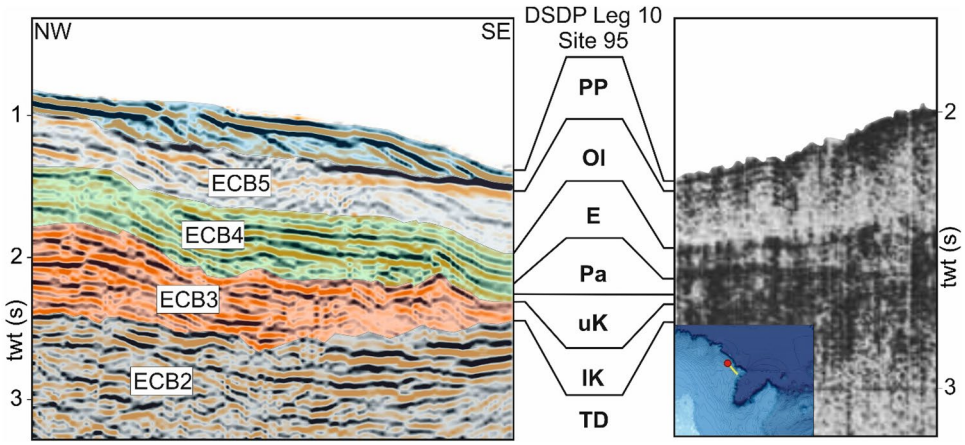

Fig. 11 Left: Vintage seismic reflection profile GT2-16 (Buffler 1977) crossing DSDP Site 95. Right: Scan of pre-site survey data for DSDP Site 95 (Worzel et al. 1973). TD: Total Depth; lK: Lower Cretaceous; uK: Upper Cretaceous; Pa: Paleocene, E: Eocene; Ol: Oligocene; PP: Pliocene–Pleistocene

et al. 2009; and references therein). ECB3 is thickest in the center of the collapsed ECB (Figs. 7 and 10), the reflection pattern is mainly chaotic and it accumulates upslope of the buttresses in the toe domain as in Figs. 7 and 9. In the toe domain and in the center of the MTD, ECB reveals internal thrusts (Fig. 7). We consequently attribute unit ECB3 to this mass transport deposits, which Paull et al. (2014) called the K-Pg Cocktail. According to the terminology by Martinez et al. (2005), the MTD is frontally emergent in Figs. 8 and 9 where the MTD runs over the buttress, but it is frontally confined in Fig. 10. Figure 8 shows that ECB3 accumulated on the terraces at the lower slope. Hence, ECB3 resembles the characteristics of the remobilized strata at the northern Campeche Bank.

The presence of the "shaken and stirred" unit ECB2 and the K-Pg Cocktail unit ECB3 along in the northern- and southernmost profiles (Figs. 5, 9) and therefore along 240 km along the ECB rim implies that these deposits are not exclusively present where a major flank collapse occurred.

Post K-Pg stratigraphy and paleoceanography

Except for the northern most profile (Fig. 5), the sediment deposits along the ECB and above unit ECB3 form a lenticular, convex sediment body, which is built by aggrading strata in the lower and basin ward prograding strata in the upper part. According to classification schemes for drifts units ECB4-9 form a typical plastered drift (e.g., Faugéres and Stow, 2008; Rebesco et al. 2014; and references therein) as already concluded for the mid Pleistocene deposits by Hübscher and Nürnberg (2023). The infill of the accommodation space that was created by the Chicxulub impact and the resulting mass wasting can be considered as an infilling drift, however, since this infilling drift has a continuous transition to the plastered drift to the north and the south, we refer to this drift as the Eastern Campeche Plastered Drift (ECPD).

In order to further constrain the stratigraphic ages of ECB4-9, we compare the reflection characteristics of individual units with those of the depositional systems on the western Florida Shelf, where stratigraphic ages were constrained by biostratigraphic markers and volcanic ash dating (Fig. 2; Gardulski et al. 1991).

As summarized in Fig. 2b, Maastrichtian to Late Oligocene deposits are aggradational on the West Florida Shelf and so is unit ECB4. Since a significant difference between the current strength between ECB and Florida is difficult to assume, we relate ECB 4 to the post K-Pg to Late Oligocene deposits. Aggradational deposition is an evidence for sedimentation in accommodation space below the deep base level. The term deep base level was coined by Hübscher et al. (2016) and describes the vertical boundary between erosion and sedimentation in subaqueous, particularly deep-water environment. The deep base level can be controlled by, e.g., bottom and contour currents (Hübscher et al. 2016; 2019), surface currents or internal waves (Qayyum et al. 2017; Hübscher and Nürnberg 2023).

When the Loop Current developed after the closure of the Suwannee Strait (Fig. 2f) and flow strength increased due to the narrowing of the CAS, prograding clinoforms developed on the West Florida Shelf until the Middle Miocene. The surface (Loop) current increase as well as the Late Oligocene eustatic sea level fall (Fig. 2i) caused therewith a relative deep base level fall that prevented sedimentation above, hence, progradation. This concept does not exclude enhanced off-bank transport by enhanced carbonate production. At the West Florida Shelf the prograding clinoforms downlapped on the topset of the Late Oligocene aggradational deposits on the West Florida Shelf (Fig. 2c). At the ECB, the unconformity that marks the transition from aggradation to progradation separates units ECB4 and ECB5 (Fig. 7). Unit ECB6 conformably overlies ECB5, so we attribute ECB5 and ECB6 to the same time interval from late Oligocene to Middle-Late Miocene during similar oceanic conditions and constant deep base level depth.

In the Middle to Late Miocene, progradational deposition transitioned back to aggradation on the West Florida Shelf (Fig. 2d). Gardulski et al. (1991) attributed this transition to a significant intensification of the Loop Current when the west-bound current into the Pacific was deflected by the shallowing of the CAS (Fig. 2h). According to these authors, the increased southward flow hampered significant off-bank transport from the Florida Shelf. The unconformity between prograding (bottom) and aggrading strata was called the Mid-Miocene Unconformity (MMU) (Gardulski et al. 1991).

The transition from progradation to aggradation is not observed on the ECB. Unit ECB7 marks a general downslope shift of deposition (Fig. 6), a decrease of aggradation and increase in progradation, and internal reflection terminate as a downlap against its basal boundary (Figs. 7, 10). Since an increase in Loop Current vigor should shift the deep base level fall further down, causing, e.g., non-deposition or truncation in water depth which were previously below the deep base leve, we associate the base of unit ECB7 with the MMU.

Since units ECB6 and ECB7 are truncated above ca. 380 m (0.5 s TWT) it cannot be reconstructed whether this units were previously aggradational further upslope. In the seismic profile in Fig. 7, the offlapping, prograding clinoforms of unit ECB8 resemble the forced regression systems tract like clinoform that was previously imaged in 4 kHz parametric sediment echosounder data by Hübscher and Nürnberg (2023).

In the northern study area, ECB7 is an upward convex drift deposit (Figs. 6, 10). In the central drift deposition unit

ECB7 forms a prograding and sigmoidal clinoform fading out downslope at 1.15 s TWT, which corresponds to ca. 860 m present day water depth (Fig. 7). The deep base level concept explains the different deposition pattern of ECB6 and ECB7. The increasing Loop Current strength pushed the deep base level down to ca. 520 m, causing erosional truncation of ECB6 and ECB7 as well as the offlapping clinoforms in Fig. 7. The falling deep base level further explains the progradation and truncation of the upper strata close to the Yucatan Strait (Figs. 8 and 9). Since these seismic units are thinner in Fig. 5, 6 and 10 and, hence, located in deeper water depths, deposition was not affected by the deep base level above.

The sigmoidal prograding unit ECB9 in Fig. 6 (see blowup) ECB9 overlies the toplapping ECB8 strata, and in Fig. 7 the ECB9 strata are onlapping. Both features document a deep base level rise. This transgressive systems tracts like unit overlies the MPUC and developed during the MPT, implying a weakening of the Loop Current since then (see Hübscher and Nürnberg 2023 for discussion).

The here proposed interaction between plate tectonics, oceanic currents and plastered drift deposition is based on a rather coarse grid of seismic profiles, constrained by jump correlation between the seismic data from this study and vintage data from the West Florida Shelf where the seismostratigraphy was constrained by core data. The lack of in situ age constrains for the ECB does not allow more detailed conclusions, but the derived explanations are consistent with finding on the conjugate shelf.

Faults, slumps and pockmarks

Several faults connect to the truncated incisions into the seafloor in Fig. 7, which implies that warping of the strata below is caused by lateral velocity variation or scattering effects, so called velocity pull-ups or push-downs (e.g., Frahm et al. 2021).

Most of the numerous near vertical faults within units ECB4-6 do not propagate to the seafloor. A plate tectonic origin of those faults is unlikely, which are not connected with deep-rooted faults. As summarized by Cartwright (2011), those layer-bound faults of a non-tectonic origin have been observed in 2D-seismic data already in the 1980s (e.g., Buckley and Grant 1985) and were interpreted as dewatering structures. By using 3D-seismic Cartwright (2004a, b) showed later that this are polygonal faults, a characteristic that we cannot test with the seismic lines of this study. Explaining the layer-bound faults purely by dewatering does not explain all observations. For example, the faults occur more frequently in the upper and lower parts of the ECPD (Figs. 5, 7). Further, Fig. 10 shows a scarp at the seafloor, below which a listric fault extends down into ECB3. Within unit ECB3, divergent reflections and overthrusts are then seen in the hangingwall domain, which suggest downslope movement. These observations suggest that the shear strength at the base of unit ECB4 or within ECB3 is so low that minor downslope creep of unit ECB4, in Fig. 7 also within ECB3 occurs, possibly simply triggered by gravitational forces. If this interpretation holds, the location of dewatering faults in the upslope domain of the creep would be facilitated by small-scale extension and by compression in the toe domain. Creep like submarine land sliding in carbonate ooze dominated drift deposits and along low-angle slopes has recently been shown by Lüdmann et al. (2021). The drift deposits in the Maldives carbonate platform as discussed by these authors show similar wavy reflection characteristics, which they attributed to ascending fluids, hence reducing the sediment shear strength. Also, this explanation is in line with the observations here.

The presence of several mass failures in our study, most pronounced in Fig. 3 and the according cross profile in Fig. 6, further corroborated the interpretation of reduced shear strength within unit ECB4. Worzel et al. (1973) concluded already from the interpretation of DSDP Leg 10 presite survey seismic data that slumping occurred throughout the Cenozoic along the ECB.

The small down warped reflections of high reflection amplitude within unit ECB8 in the northernmost profile (Fig. 5) are typical for buried gas escape structures, so called pockmarks (Hovland and Judd 1988). Multibeam data that were collected along that profile show pockmarks also on the seafloor (Hübscher and Nürnberg 2023). Analysis of satellite synthetic aperture radar mapping showed oils and gas seepage on the sea surface at the southern ECB (Kennicut 2017), so it is very likely that active hydrocarbons escape started at the ECB during deposition of units ECB8-9 and the Pleistocene, respectively. Pockmarks on carbonate platforms has been previously observed, e.g., at the Maldives (Betzler et al. 2011). We can just speculate that the source rock is part of the Oxfordian (Upper Jurassic) hydrocarbon system, which according to Hood et al. (2002) is the southernmost source rock in the Gulf of Mexico. The organic matter deposited during Oceanic Anoxic Events (Schlanger and Jenkyns 1976) may offer be considered as potential sources. The escape of fluids on the sea floor needs further attention, since expelling hydrocarbons may influence water chemistry as well as flora and fauna habitats (Judd and Hovland 2009; Idczak et al. 2020).

Conclusions

We present the first detailed seismic reflection seismic study of the deep-sea record of the Chicxulub impact at the K-Pg boundary and the oceanic current controlled depositional evolution of a plastered drift on the ECB. The seismic wave induced by the Chicxulub impact caused

the collapse of the ECB over a length of ca. 200 km, hence creating accommodation space for the ECPD. The internal structure of Upper Cretaceous strata was disintegrated. The failed material was partly transported downslope. Another part remained on the decollement and formed in dependency of the presence and height of a buttress a frontally confined or frontally emergent mass transport deposit. The observation of these processes, that were previously observed at the northern Campeche Bank only, documents the devasting energy that a meteorite impact induces into the earth system.

The closure of the Suwannee Strait in the Late Oligocene and the shallowing and later on the closure of the CAS in the Mid to Late Miocene controlled the Loop Current variability in space and time, which in turn controlled the deep base level and therewith the transition from aggradational to progradational deposition of the ECPD. The deep base level concept proved to be a useful tool for explaining depositional pattern on continental slope.

Since the Loop Current transports heat from the western Atlantic warm water pool into the North Atlantic, from where heat and moisture is forwarded to NW Europe by the Gulf Stream, the ECPD represents an archive for the paleoenvironment of the northern hemisphere. The disclosure of this East Campeche Bank archive needs future attention by interdisciplinary earth system researchers.

Supplementary Information The online version contains supplementary material available at https://doi.org/10.1007/s11001-023-09514-3.

Acknowledgements We like to thank captain Michael Schneider, his officers and crew of RV METEOR for their support of ship based working program. We further like to thank Wolfgang Mahrle (German Federal Foreign Office), Mr. Hubertus von Römer (German Embassy Mexico City) and Mr. Ansgar Sittman (German Embassy Washington) for their great support during the diplomatic clearance. Jonas Preine is thanked for proof reading as well as Chris Lowery and Sean Gulick for discussions at the early stage of this study.

Authors contributions CH and TH wrote the manuscript. CB significantly contributed to the scientific evaluation of the discussed data. CK and BW also contributed to the interpretation and supervised data acquisition. All authors reviewed and agreed to co-author this manuscript.

Funding Open Access funding enabled and organized by Projekt DEAL. RV METEOR expedition M94 was funded by the German Research Foundation (DFG) and the Federal Ministry of Education and Research (BMBF).

Data availability All M94 seismic data are uploaded as SEG-Y to PANGAEA data base and will be made public including DOI directly after publication.

Declarations

Competing interests The authors declare that they have no known competing financial interests or personal relationships that could have appeared to influence the work reported in this paper.

References

Alvarez LW, Alvarez W, Asaro F, Michel HV (1980) Extraterrestrial cause for the cretaceous-tertiary extinction. Science 208(4448):1095–1108

Antoine JW, Ewing JI (1963) Seismic refraction measurements on the margins of the Gulf of Mexico. J Geophys Res 68:1975–1996

Betzler C, Lindhorst S, Hübscher C, Lüdmann T, Fürstenau J (2011) Giant pockmarks in a carbonate platform (Maldives, Indian Ocean). Mar Geol 289:1–16

Buckley DE, Grant AC (1985) Fault like features in abyssal plain sediments: possible dewatering structures. J Geophys Res 90:9173–9180

Buffler RT, Schleger W, Bowdler JB, Party S (1984) Initial Report of the Deep Sea Drilling Project, Leg 77. Scripps institution Oceanography, CA, Washington, p 77

Buffler RT (1977) Gulf tectonics phase 2. data retrieved from the IDA Green Expedition 2302, https://www.marine-geo.org/tools/datasets/28390.

Bull S, Cartwright J, Huuse M (2009) A review of kinematic indicators from mass-transport complexes using 3d seismic data. Mar Pet Geol 26(7):1132–1151

Cartwright JA (1994a) Episodic basin-wide hydrofracturing of overpressured early Cenozoic mudrock sequences in the North Sea Basin. Mar Pet Geol 11:587–607

Cartwright JA (1994b) Episodic basin-wide fluid expulsion from geopressured shale sequences in the North Sea Basin. Geology 22:447–450

Cartwright J (2011) Diagenetically induced shear failure of fine-grained sediments and the development of polygonal fault systems. Mar Pet Geol 28:1593–1610

Christeson GL, Van Avedndonk HJA, I.Norton O, Snedden JW, Eddy DR, Karner GD, Johnson CA (2014) Deep crustral structure in the eastern Gulf of Mexico. J Geophys Res 119:6782–6801

Covey C, Thompson SL, Weissman PR, MacCracken MC (1994) Global climatic effects of atmospheric dust from an asteroid or comet impact on earth. Glob Planet Chang 9(3):263–273

Day S, Maslin M (2005) Linking large impacts, gas hydrates, and carbon isotope excursions through widespread sediment liquefaction and continental slope failure: the example of the K-T boundary event. In: Kenkmann T, Hörz F, Deutsch A (eds) Large meteorite impacts III. Geological Society of America, Boulder

Dillon, WP, Paull, CK, Buffler, RT, and Fail, J-P (1979) Structure and development of the Southeast Georgia Embayment and northern Blake Plateau; preliminary analysis. In: Watkins JS, Montadert L, Dickerson PW (eds) Geological and geophysical investigations of continental margins: American Association of Petroleum Geologists (AAPG) Memoir 29

Eddy DR, Van Avendonk HJA, Christeson GL, Norton IO, Karner GD, Johnson CA, Snedden JW (2014) Deep crustal structure of the northeastern Gulf of Mexico: implications for rift evolution and seafloor spreading. J Geophys Res Solid Earth 119:6802–6822

Faugères J-C, Stow DAV (2008) Contourite drifts: nature, evolution and controls. In: Contourites Rebesco M, Camerlenghi A (eds) Developments in Sedimentology, vol 60, pp 257–288. Elsevier, Amsterdam

Frahm L, Hübscher C, Warwel A, Preine J, Huster H (2020) Misinterpretation of velocity pull-ups caused by high-velocity infill of tunnel valleys in the southern Baltic Sea. Near Surf Geophys 18(6):643–657. https://doi.org/10.1002/nsg.12122

Gardulski AF, Marguerite HG, Milsark A, Weiterman SD, Sherwood WW Jr, Mullins HT (1991) Evolution of a deep-water carbonate platform: upper Cretaceous to Pleistocene sedimentary environments on the west Florida margin. Mar Geol 101:163–179

Guzmán-Hidalgo E, Grajales-Nishimura JM, Eberli GP, Aguayo-Camargo JE, Urrutia-Fucugauchi J, Pérez-Cruz L (2021) Seismic stratigraphic evidence of a pre-impact basin in the Yucatán Platform: morphology of the Chicxulub crater and K/Pg boundary deposits. Mar Geol 441:106594

Hildebrand AR, Penfield GT, Kring DA, Pilkington M, Camargo ZA, Jacobsen SB, Boynton WV (1991) Chicxulub Crater: a possible Cretaceous/Tertiary boundary impact crater on the Yucatan Peninsula. Mex Geol 19(9):867–871

Hildebrand AR, Pilkington M, Ortiz-Aleman C, Chavez RE, Urrutia-Fucugauchi J, Connors M, Graniel-Castro E, Camara-Zi A, Halpenny JF, Niehaus D (1998) Mapping chicxulub crater structure with gravity and seismic reflection data. Geol Soc 140(1):155–176

Hood KC, Wenger LM, Gross OP, Harrison SC (2002) Hydrocarbon systems analysis of the northern Gulf of Mexico: delineation of hydrocarbon migration pathways using seeps and seismic imaging. In: Schumacher D, LeSchack LA (eds) AAPG studies in geology No. 48 and SEG Geophysical References Series 11:25–40

Hovland M, Judd AG (1988) Seabed pockmarks and seepages: impact on geology, biology and the marine environment, vol 293. Graham & Trotman, London

Hübscher C, Gohl K (2014) Reflection/refraction seismology. Encyclopedia of marine geosciences. Springer, New York. https://doi.org/10.1007/987-94-007-6644-0_128-1

Hübscher C, Nürnberg D (2023) Loop current attenuation after the Midpleistocene transition contributes to northern hemisphere cooling. Mar Geol 456:106976. https://doi.org/10.1016/j.margeo.2022.106976

Hübscher C, Dullo C, Flögel S, Titschack J, Schönfeld J (2010) Contourite drift evolution and related coral growth in the eastern Gulf of Mexico and its gateways. Int J Earth Sci. https://doi.org/10.1007/s00531-010-0558-6

Hübscher C, Nürnberg D, Al Hseinat M, Alvarez García M, Erdem Z, Gehre N, Jentzen A, Kalvelage C, Karas C, Kimmel B, Mildner T, Ortiz AO, Parker AO, Petersen A, Raeke A, Reiche S, Schmidt M, Weiß B, Wolf D (2014) Yucatan throughflow—Cruise No. M94—March 12–March 26, 2013—Balboa (Panama)—Kingston (Jamaica). METEOR Berichte, M94, 32 pp, DFG-Senatskommission für Ozeanographie. https://doi.org/10.2312/cr_m94

Hübscher C, Betzler C, Reiche S (2016) Seismo-stratigraphic evidences for deep base level control on middle to late Pleistocene drift evolution and mass wasting along southern Levant continental slope (Eastern Mediterranean). J Mar Pet Geol 77:526–534

Hübscher C, Al Hseinat M, Schneider M, Betzler C (2019) Evolution of Contourite Systems in the Late Cretaceous Chalk Sea along the Tornquist Zone. Sedimentology 66:1341–1360

Idczak J, Brodecka-Goluch A, Łukawska-Matuszewska K, Graca B, Gorska N, Klusek Z, Pezacki PD, Bolałek J (2020) A geophysical, geochemical and microbiological study of a newly discovered pockmark with active gas seepage and submarine groundwater discharge (MET1-BH, central Gulf of Gdańsk, southern Baltic Sea). Sci Total Environ 742:140306

Judd A, Hovland M (2009) Seabed fluid flow: the impact on geology, biology and the marine environment. Cambridge University Press, Cambridge

Kennicutt MC (2017) Oil and gas seeps in the Gulf of Mexico. In: Ward CH (ed) Habitats and biota of the Gulf of Mexico: before the deep water horizon spill. Doi: https://doi.org/10.1007/978-1-4939-3447-8_5. pp 275–358

Kinsland GL, Egedahl K, Strong MA, Ivy R (2021) Chicxulub impact tsunami megaripples in the subsurface of Louisiana: Imaged in petroleum industry seismic data. Earth Planet Sci Lett 570:117063

Kneller EA, Jackson CA (2011) Plate kinematics of the Gulf of Mexico based on integrated observations from the Central and South Atlantic. GCAGS Trans 61:283–299

Logan BW, Harding JL, Ahr WM, Williams JD, Snead RG (1969) Late Quaternary sediments of Yucatan Shelf, Mexico. In: Carbonate sediments and reefs, vol 11. Yucatan Shelf, Mexico. AAPG Memoir, pp 5–128

Lüdmann T, Betzler C, Lindhorst S, Lahajnar N, Hübscher C (2022) Submarine landsliding in carbonate ooze along low-angle slopes (Inner Sea, Maldives). Mar Pet Geol 136:105403. https://doi.org/10.1016/j.marpetgeo.2021.105403

Martinez JF, Cartwright J, Hall B (2005) 3D seismic interpretation of slump complexes: examples from the continental margin of Israel. Basin Res 17:83–108. https://doi.org/10.1111/j.1365-2117.2005.00255.xr2005

Mickus K, Stern RJ, Keller G, Anthony EY (2009) Potential field evidence for a volcanic rifted margin along the Texas Gulf Coast. Geology 37:387–390

Mullins HT, Gardulski AF, Wise SW Jr, Applegate J (1987) Middle Miocene oceanogrpahic event in the eastern Gulf of Mexico: implications for seismic stratigraphic succession and Loop Current/Gulf Stream circulation. Geol Soc Am Bull 98:702–713

Mullins HT, Gardulski AF, Hine AC, Melillo AJ, Wise SW, Applegate J (1988) Three-dimensional sedimentary framework of the carbonate ramp slope of central west Florida: a sequential seismic stratigraphic perspective. Geol Soc Am Bull 100:514–533

Newkirk DR, Martin EE (2009) Circulation through the Central American Seaway during the Miocene carbonate crash. Geology 37:87–90

O'Dea et al (2016) Formation of the Isthmus of Panama. Sci Adv 2(8):e1600883

Oey LY (2008) Loop Current and deep eddies. J Phys Oceanogr 38:1426–1447

Ordonez E (1936) Principal physiogeographic provinces of Mexico. Am Assoc Petrol Geol Bull 20:1277–1307

Osborne AH, Newkirk DR, Groeneveld J, Martin EE, Tiedemann R, Frank M (2014) The seawater neodymium and lead isotope record of the final stages of Central American Seaway closure. Paleoceanography 29:715–729

Paull CK, Caress DW, Gwiazda R, Urrutia-Fucugauchi J, Rebolledo-Vieyra M, Lundsten E, Anderson K, Sumner EJ (2014) Cretaceous-Paleogene boundary exposed: Campeche Escarpment, Gulf of Mexico. Mar Geol 357:392–400. https://doi.org/10.1016/j.margeo.2014.10.002

Pindell JL, Kennan L (2009) Tectonic evolution of the Gulf of Mexico, Caribbean and northern South America in the mantle reference frame: an update. Geol Soc 328:1–55

Poag CW (2017) Shaken and stirred: Seismic evidence of Chicxulub impact effects on the West Florida carbonate platform, Gulf of Mexico. Geology 45:1011–1014. https://doi.org/10.1130/G39438.1

Purser BH (1983) Sédimentation et diagenèse des carbonates néritiques récents, vol 2. IFP, Ed. Technip

Qayyum F, Betzler C, Catuneanu O (2017) The Wheeler diagram, flattening theory, and time. Mar Pet Geol 86:1417–1430

Randazzo AF (1997) The sedimentary platform of Florida: Mesozoic to Cenozoic. In: Randazzo AF, Jones DS (eds) The geology of Florida. University Press of Florida, Gainesville, pp 39–56

Rebesco M, Hernández-Molina FJ, van Rooij D, Wahlin A (2014) Contourites and associated sediments controlled by deep-water circulation processes: state-of the-art and future considerations. Mar Geol 352:111e154

Renne PR, Deino AL, Hilgen FJ, Kuiper KF, Mark DF, Mitchell WS III, Morgan LE, Mundil R, Smit J (2013) Time scales of critical events around the Cretaceous-Paleogene boundary. Science 339(6120):684–687. https://doi.org/10.1126/science.1230492

Sanford JC, Snedden JW, Gulick SPS (2016) The Cretaceous-Paleogene boundary deposit in the Gulf of Mexico: Large-scale oceanic basin response to the Chicxulub impact. J Geophys Res Solid Earth 121:1240–1261. https://doi.org/10.1002/2015JB012615

Schlager W, Buffler RT, Angstadt D, Phair R (1984) Geologic history of the southeastern Gulf of Mexico. In: Buffler RT, Schlager W, Leg 77 Science Party (es) Initial Reports of the Deep Sea Drilling Project, Leg 77. Washington, Scripps institution Oceanography, CA

Schlanger S, Jenkyns H (1976) Cretaceous oceanic anoxic events: Causes and consequences. Geologie En Mijnbouw 55(3-4):179–84

Schulte P et al (2010) The Chicxulub asteroid impact and mass extinction at the Cretaceous-Paleogene boundary. Science 327(5970):1214–1218. https://doi.org/10.1126/science.1177265

Sheinbaum J, Candela J, Badan A, Ochoa J (2002) Flow structure and transport in the Yucatan Channel. Geophys Res Lett 29(3):1040. https://doi.org/10.1029/2001GL013990

Uchupi E, Emery KO (1968) Structure of continental margin off Gulf Coast of United States. Am Assoc Petrol Geol Bull 52:1162–1193

Van Avendonck HJA, Christeson GL, Norton IO, Eddy DR (2015) Continental rifting and sediment infill in the northwestern Gulf of Mexico. Geology 43(7):631–634. https://doi.org/10.1130/G36798.1

Worzel J, Buffler RT (1978) Gulf tectonics phase 3. Data retrieved from the IDA Green Expedition 2801, https://www.marine-geo.org/tools/datasets/28447

Worzel J L, Bryant W and Shipboard Scientific Party (1973) Site 95. In: Worzel JL, Bryant W and Scientific Party, Initial Reports of the Deep Sea Drilling Project, Volume X, Washington (U.S. Government Printing Office), 259–295